

Article

An Update on Eukaryotic Viruses Revived from Ancient Permafrost

Jean-Marie Alempic ^{1,†}, Audrey Lartigue ^{1,†}, Artemiy E. Goncharov ² , Guido Grosse ^{3,4} , Jens Strauss ³, Alexey N. Tikhonov ⁵, Alexander N. Fedorov ⁶ , Olivier Poirot ¹ , Matthieu Legendre ¹ , Sébastien Santini ¹ , Chantal Abergel ¹  and Jean-Michel Claverie ^{1,*} 

¹ IGS, Information Génomique & Structurale (UMR7256), Institut de Microbiologie de la Méditerranée (FR 3489), Institut Microbiologie, Bioénergies et Biotechnologie, and Institut Origines, CNRS, Aix Marseille University, 13288 Marseille, France

² Department of Molecular Microbiology, Institute of Experimental Medicine, Department of Epidemiology, Parasitology and Disinfectology, Northwestern State Medical Mechnikov University, Saint Petersburg 195067, Russia

³ Permafrost Research Section, Alfred Wegener Institute, Helmholtz Centre for Polar and Marine Research, 14473 Potsdam, Germany

⁴ Institute of Geosciences, University of Potsdam, 14478 Potsdam, Germany

⁵ Laboratory of Theriology, Zoological Institute of Russian Academy of Science, Saint Petersburg 199034, Russia

⁶ Melnikov Permafrost Institute, Yakutsk 677010, Russia

* Correspondence: jean-michel.claverie@univ-amu.fr; Tel.: +33-413-946-777

† These authors contributed equally to this work.

Abstract: One quarter of the Northern hemisphere is underlain by permanently frozen ground, referred to as permafrost. Due to climate warming, irreversibly thawing permafrost is releasing organic matter frozen for up to a million years, most of which decomposes into carbon dioxide and methane, further enhancing the greenhouse effect. Part of this organic matter also consists of revived cellular microbes (prokaryotes, unicellular eukaryotes) as well as viruses that have remained dormant since prehistorical times. While the literature abounds on descriptions of the rich and diverse prokaryotic microbiomes found in permafrost, no additional report about “live” viruses have been published since the two original studies describing pithovirus (in 2014) and mollivirus (in 2015). This wrongly suggests that such occurrences are rare and that “zombie viruses” are not a public health threat. To restore an appreciation closer to reality, we report the preliminary characterizations of 13 new viruses isolated from seven different ancient Siberian permafrost samples, one from the Lena river and one from Kamchatka cryosol. As expected from the host specificity imposed by our protocol, these viruses belong to five different clades infecting *Acanthamoeba* spp. but not previously revived from permafrost: Pandoravirus, Cedratvirus, Megavirus, and Pacmanvirus, in addition to a new Pithovirus strain.

Keywords: permafrost; *Acanthamoeba*; giant virus; Pleistocene; Siberia; Kamchatka



Citation: Alempic, J.-M.; Lartigue, A.; Goncharov, A.E.; Grosse, G.; Strauss, J.; Tikhonov, A.N.; Fedorov, A.N.; Poirot, O.; Legendre, M.; Santini, S.; et al. An Update on Eukaryotic Viruses Revived from Ancient Permafrost. *Viruses* **2023**, *15*, 564. <https://doi.org/10.3390/v15020564>

Academic Editor: David D. Dunigan

Received: 27 October 2022

Revised: 2 February 2023

Accepted: 10 February 2023

Published: 18 February 2023



Copyright: © 2023 by the authors. Licensee MDPI, Basel, Switzerland. This article is an open access article distributed under the terms and conditions of the Creative Commons Attribution (CC BY) license (<https://creativecommons.org/licenses/by/4.0/>).

1. Introduction

Ongoing international modeling and monitoring studies keep confirming that the continuous release of greenhouse gas (mostly CO₂) due to human activities since the industrial revolution is causing significant climate change through global warming. It is now widely acknowledged that an average temperature increase of 1.5 °C relative to 1850–1900 would be exceeded during the 21st century, under all realistic circumstances [1] even though the adequacy of present climate models to predict regional changes remains in debate [2]. For instance, climate warming is particularly noticeable in the Arctic where average temperatures appear to increase more than twice as fast as in temperate regions [3]. One of the most visible consequences is the global thawing of permafrost at increasing depths [4,5], the rapid erosion of permafrost bluffs [6,7], as well as erosion of deep and old permafrost by thaw slumping in hillslopes [8,9]. This rapid permafrost thaw causes

mobilization of ancient organic matter previously preserved for millennia in permafrost deep layers, a phenomenon most visible in Siberia, where deep continuous permafrost underlays most of the North Eastern territories.

The thawing of permafrost has significant microbiological consequences. First, above freezing temperatures, the return of liquid water triggers the metabolic reactivation of numerous soil microorganisms (bacteria, archaea, protists, fungi) [10–14], exposing the organic material previously trapped in permafrost to decomposition, releasing additional CO₂ and methane further contributing greenhouse gas to the atmosphere [5,15,16]. Yet, a more immediate public health concern is the physical release and reactivation of bacteria (or archaea) that have remained in cryptobiosis trapped in deep permafrost, isolated from the Earth's surface for up to two million years [10,17] (although a more consensual limit would be half a million years [18]). On a shorter time scale, the periodical return of anthrax epidemics devastating reindeer populations has been linked to the deeper thawing of the permafrost active layer at the soil surface during exceptionally hot summers, allowing century-old *Bacillus anthracis* spores from old animals burial grounds or carcasses to resurface [19–21].

One could imagine that very deep permafrost layers (i.e., million-year-old), such as those extracted by open-pit mining, could release totally unknown pathogens [22]. Finally, the abrupt thawing vertically operating along the whole wall of permafrost bluffs (consisting of specific ice-rich deposits called “yedoma”) such as seen in the Kolyma lowland or around the Yukon River, Alaska, causes the simultaneous release of ancient microorganisms from frozen soils dating from the whole Holocene to the late Pleistocene (i.e., up to 120,000 years ago) [23]. Many culture-based and culture-independent studies (i.e., barcoding and/or metagenomics) have documented the presence of a large diversity of bacteria in ancient permafrost [10–12,17,24–28], a significant proportion of which are thought to be alive, although estimates vary greatly with the depth (age) and soil properties [17,29,30]. These bacterial populations include relatives of common contemporary pathogens (*Acinetobacter*, *Bacillus anthracis*, *Brucella*, *Campylobacter*, *Clostridia*, *Mycoplasma*, various *Enterobacteria*, *Mycobacteria*, *Streptococci*, *Staphylococci*, *Rickettsia*) [11,12,24,29,31]. Fortunately, we can reasonably hope that an epidemic caused by a revived prehistoric pathogenic bacterium could be quickly controlled by the modern antibiotics at our disposal, as they target cellular structures (e.g., ribosomes) and metabolic pathways (transcription, translation or cell wall synthesis) conserved during the evolution of all bacterial phyla [32], even though bacteria carrying antibiotic-resistance genes appear to be surprisingly prevalent in permafrost [26,31,33].

The situation would be much more disastrous in the case of plant, animal, or human diseases caused by the revival of an ancient unknown virus. As unfortunately well documented by recent (and ongoing) pandemics [34,35], each new virus, even related to known families, almost always requires the development of highly specific medical responses, such as new antivirals or vaccines. There is no equivalent to “broad spectrum antibiotics” against viruses, because of the lack of universally conserved druggable processes across the different viral families [36,37]. It is therefore legitimate to ponder the risk of ancient viral particles remaining infectious and getting back into circulation by the thawing of ancient permafrost layers. Focusing on eukaryote-infecting viruses should also be a priority, as bacteriophages are no direct threat to plants, animals, or humans, even though they might shape the microbial ecology of thawing permafrost [38].

Our review of the literature shows that very few studies have been published on this subject. To our knowledge, the first one was the isolation of Influenza RNA from one frozen biopsy of the lung of a victim buried in permafrost since 1918 [39] from which the complete coding sequence of the hemagglutinin gene was obtained. Another one was the detection of smallpox virus DNA in a 300-year-old Siberian mummy buried in permafrost [40]. Probably for safety/regulatory reasons, there were not follow-up studies attempting to “revive” these viruses (fortunately). The first isolation of two fully infectious eukaryotic viruses from 30,000-y old permafrost was thus performed in our laboratory

and published in 2014 and 2015 [41,42]. A decisive advantage of our approach was to choose *Acanthamoeba* spp. as a host, to act as a specific bait to potentially infectious viruses, thus eliminating any risk for crops, animals, or humans. However, no other isolation of a permafrost virus has been published since, which might suggest that these were lucky shots and that the abundance of viruses remaining infectious in permafrost is very low. This, in fact, is wrong, as numerous other *Acanthamoeba*-infecting viruses have been isolated in our laboratory, but not yet published pending their complete genome assembly, annotation, or detailed analysis. In the present article, we provide an update on thirteen of them, most of which remain at a preliminary stage of characterization. These isolates will be available for collaborative studies upon formal request through a material transfer agreement. The ease with which these new viruses were isolated suggests that infectious particles of viruses specific to many other untested eukaryotic hosts (protozoans or animals) probably remain abundant in ancient permafrost.

2. Materials and Methods

2.1. Permafrost Sampling

The various on-site sampling protocols have been previously described in [31,43] for samples #3 and #5 (collected in the spring 2015), in [13,44] for sample #4, in [45] for sample #6, and [46,47] for samples #7–9 (see Table 1).

Table 1. Samples and virus description.

Sample #	GPS Coordinates	Description	Isolated Virus
1	55°06'54" N 159°57'48" E	Surface soil, Shapina river bank, Kamchatka Modern	<i>Cedratovirus kamchatka</i> (strain P5)
2	62°06'23.92" N 129°48'35" E	Lena river, Yakutsk Modern	<i>Cedratovirus lena</i> (strain DY0) <i>Pandoravirus lena</i> (strain DY0)
3	61°45'39.1" N E 130°28'28.78"	Talik, −6.5 m below a lake, Yukechi Alas [43] Isolation: >53 y BP	<i>Pandoravirus talik</i> (strain Y4)
4	68°38'21.1" N 159°3'20.67" E	Melting ice wedge Duvanny yar [23,44] Mixed ages	<i>Cedratovirus duvanny</i> (strain DY1) <i>Pandoravirus duvanny</i> (strain DY1)
5	61°45'39.1" N 130°28'28.78" E	−16 m below a lake, Yukechi Alas [43] Isolation: >48,500 y BP	<i>Pandoravirus yedoma</i> (strain Y2)
6	74°13'00" N 141°03'48" E	Woolly mammoth stomach content, Maly Lyakhovskiy Island [45] Isolation: >28,600 y BP	<i>Pandoravirus mammoth</i> (strain Mm38)
7	70°43'25" N 135°25'47" E	Soil with mammoth wool RHS paleolithic site, Yana river left bank [46,47] Isolation: >27,000 BP	<i>Megavirus mammoth</i> (strain Yana14) <i>Pithovirus mammoth</i> (strain Yana14) <i>Pandoravirus mammoth</i> (strain Yana14)
8*	70°43'25" N 135°25'47" E	Fossil wolf (<i>Canis lupus</i>) intestinal content, RHS paleolithic site [46,47] Isolation: >27,000 y BP	<i>Pandoravirus lupus</i> (strain Tums1)
9*	70°43'25" N 135°25'47" E	Fossil wolf (<i>Canis lupus</i>) intestinal content, RHS paleolithic site [46,47] Isolation: >27,000 y BP	<i>Pacmanvirus lupus</i> (strain Tums2)

* Same location, but different frozen remains.

Liquid samples #2 and #4 were collected in pre-sterilized 50 mL Falcon tube in August 2019, as well as sample #1 consisting of surface soil without vegetation from the Shapina river bank, collected on 07/15/2017 and since maintained frozen at -20°C in the laboratory.

2.2. Sample Preparation for Culturing

About 1 g of sample was resuspended in 40 mM Tris pH 7.5, from 2–10% *v/v* depending on its nature (liquid, mud, solid soil) and vortexed at room temperature. After decanting for 10 min, the supernatant was taken up, then centrifugated at $10,000\times g$ for one hour. The pellet was then resuspended in 40 mM Tris pH 7.5 with a cocktail of antibiotics (Ampicillin 100 $\mu\text{g}/\text{mL}$, Chloramphenicol 34 $\mu\text{g}/\text{mL}$, Kanamycin 20 $\mu\text{g}/\text{mL}$). This preparation was then deposited one drop at a time onto two 15 cm-diameter Petri dishes (Sarsted 82.1184.500), one previously seeded with *Acanthamoeba castellanii* (Douglas) Neff (ATCC 30010TM) at 500 cells/ cm^2 , the other with *A. castellanii* cells previously adapted to Fungizone (Amphotericin B, Gibco, Pasley, UK) by serial passages in presence of increasing concentration of the drug up to 2.5 $\mu\text{g}/\text{mL}$. Fungizone was used to inhibit the proliferation of viable microfungi known to be present in permafrost.

2.3. Detection of Virus Infection

Changes in the usual appearance of *A. castellanii* cells (rounding up, non-adherent cells, encystment, change in vacuolization and/or refractivity) might eventually have become visible after 72 h, but might have been due to a variety of irrelevant causes such as overconfluency, the presence of a toxin, or the proliferation of bacteria or microfungi. Under a light microscope, the areas exhibiting the most visible changes were spotted using a p1000 pipetman. This 1 mL volume was then centrifugated ($13,000\times g$ for 30 min), the pellet resuspended in 100 μL and scrutinized under a light microscope. This subsample was also used to seed further T25 cell culture flasks of fresh *A. castellanii* cells.

2.4. Preliminary Identification of Infecting Viruses

Potential viral infections are suggested by intracellular changes (presence of cytoplasmic viral factories, nuclear deformation, lysis), or by the direct visualization of giant virus particles. Using a set of in-house-designed family-specific primers (Table 2), a PCR test was performed using the Terra PCR Direct Polymerase Mix (Takara Bio Europe SAS, Saint-Germain-en-Laye, France). Amplicons were then sequenced (Eurofins Genomics, Ebersberg, Germany) to confirm the presence of new isolates of a given acanthamoeba-infecting virus family (Table 2) suggested by their particle morphology and ultrastructural features.

Table 2. PCR primers used to identify the newly isolated viruses.

Virus Family or Subgroup	Primer Sequences (Forward & Reverse)	Prototype Gene
<i>Pandoraviridae</i>	F: TCGTGGATCGACATTGGCGTGCAGTT R: CTGGTAGGTGACGGCAAAGTT	<i>Pandoravirus salinus</i> (NC_022098) CDS_1260 Putative oxidoreductase
<i>Cedratvirus</i>	F: AAACCTAGGTTGCTAACTGTAGATCCTTG R: GGAACCAGCGTTACCGAGTGCATCTTC	<i>Cedratvirus A11</i> (NC_032108) BQ3484_149 Hypothetical protein
<i>Pithoviridae</i>	F: GTGGTCCAAAACCTGGAAGAATA R: GCGTCAAGCTCAACATCAAGTTC	<i>Pithovirus sibericum</i> (NC_023423) pv_393 DNA/RNA helicase
<i>Megavirinae</i> (A, B, C lineages)	F: TGAATAATGGTGATGGTATTGATGT R: ACTGGTACCTAATCCTTTGTAATATTT	<i>M. chilensis</i> (NC_016072) mg403 Topoisomerase 2
<i>Pacmanvirus</i>	F: GTCTCAATGGGCCACTTGAGCTG R: CCCGCTCTTGACCTCTGGGTTC	<i>Pacmanvirus A23</i> (LT706986) PACV_217 Major Capsid Protein

2.5. Nomenclature of New Isolates

We used the binomial format for the naming of virus species, where the genus name and a species epithet together form a unique species name. The genus name (e.g., “Pithovirus”) was attributed on the basis of concordant similarities with previously characterized amoeba-infecting viruses: genome sequences (PCR amplification using specific probes, partial or complete genome sequences), cell-infection patterns, and virion morphological features. The species epithet was chosen to reflect the location or nature of the source sample (e.g., “duvanny”). A strain name (e.g., “Tums1”) was added to further specify the precise sample (there might be several from the same location/source) from which the isolation was performed. Strain names can thus be shared by different species.

2.6. Further Characterization of New Virus Isolates

Positive subcultures are then reseeded and passaged in T25 then T75 cell culture flasks (Nunc™ EasYFlasks™, ThermoFisher scientific, Waltham, MA, USA) until the density/quantity of viral particles allows their further characterization by Transmission Electron Microscopy (TEM). New viral isolates of particular interest are then eventually cloned and their whole genome sequenced. The relationship of the new isolates to the other members of their cognate family was estimated using a phylogenetic clustering of the DNA-directed RNA polymerase largest subunit (RPB1) orthologous sequences. RPB1 is recognized as a convenient phylogenetic classifier for the nucleocytoplasmic large DNA viruses (phylum *Nucleocytoviricota*) [48].

2.7. Viral Genome Sequencing

Virus cloning, virus particles purification using a cesium chloride gradient, and DNA extraction from approximately 5×10^9 purified particles (using the Purelink Genomic extraction mini kit, ThermoFisher) have been previously described [49]. Sequence data were generated from the Illumina HiSeq X platform provided by Novogene Europe (Cambridge, UK). Genome data assembly was performed in-house as previously described [49].

2.8. Deposition of Sequences

The partial or complete genome sequences of 8 new virus isolates determined in this work have been deposited in Genbank, with accession numbers as follows:

- *Pandoravirus talik* (strain Y4): OQ413801
- *Pandoravirus lena* (strain DY0): OQ411594-OQ411599
- *Pandoravirus mammoth* (strain Mm38): OQ411600-OQ411601
- *Megavirus mammoth* (strain Yana14): OQ411602
- *Pithovirus mammoth* (strain Yana14): OQ413582
- *Cedratvirus duvanny* (strain DY1): OQ413581
- *Cedratvirus lena* (strain DY0): OQ413577-OQ413579, OQ41358
- *Pacmanvirus lupus* (strain Tums2): OQ411603

2.9. Design of Virus-Specific PCR Primers

Clusters of protein-coding genes common to all known members of a viral family or clade were identified using Orthofinder [50]. The protein sequence alignments of these clusters were converted into nucleotide alignments using Pal2nal [51]. Statistics on the multiple alignments were then computed using Alistat [52] and sorted using the “most unrelated pair criteria”. The corresponding alignments were thus visually inspected to select the variable regions flanked by strictly conserved sequences suitable as PCR primers. The primers and their genes of origin are listed in Table 2.

3. Results

3.1. Pandoraviruses

Seven of the 13 new virus isolates reported in the present article were found to be new members of the Pandoraviridae family. Observed under the light microscope during the

early phase of the isolation process, their proliferation in acanthamoeba cultures generated inhomogeneous populations of large ovoid particles (up to 1 µm in length and 0.5 µm in diameter). As for known pandoraviruses, the infection of *A. castellanii* cells was initiated by the internalization of individual particles via phagocytic vacuoles. Eight to 10 h after infection, the Acanthamoeba cells become rounded, lose their adherence, and new particles appear in the cytoplasm. The replicative cycle ends with the cells lysis releasing about a hundred particles each. Using TEM, the particles appeared enclosed in a 70-nm thick electron-dense tegument with a lamellar structure parallel to the particle surface and interrupted by an ostiole-like apex (Figure 1A). In complement to these morphological features unique to the Pandoraviridae [53], PCR tests were performed to confirm the identification of the new isolates using family-specific sets of primers (Table 2) and the amplicons sequenced to evaluate their genetic divergence with other members of the family (Table 3). All new isolates were found to be significantly distinct from each other and from contemporary strains, albeit within the range of divergence (93–86% nucleotide identity) previously observed (Table 3). Among these new isolates, four originated from radiocarbon-dated ancient permafrost: *Pandoravirus yedoma* (strain Y2) (>48,500 y BP), *P. mammoth* (strain Mm38) (>28,600 y BP), *P. mammoth* (strain Yana14) (>27,000 y BP), and *P. lupus* (strain Tums1) (>27,000 y BP). One originated from an unfrozen permafrost layer: *P. talik* (strain Y4), one from a melted mixture of permafrost layers (*P. duvanny* (strain DY1), and one from the muddy bank of the Lena river: *P. lena* (strain DY0). Draft genomic sequences were determined for *P. lena*, *P. talik*, and *P. mammoth* (strain Mm38). Their large sizes fall in the range of previously sequenced pandoraviruses (Table 3). A clustering of *P. duvanny*, *P. lena*, *P. talik*, and *P. mammoth* (strain Mm38) within the Pandoraviridae family is shown in Figure 2.

Table 3. PCR identification of previous and new Pandoravirus isolates.

Virus	Accession	Base Pairs (Contigs)	Amplicon Identity *
<i>Pandoravirus salinus</i> (prototype)	NC_022098	2,473,870	100% (1203/1203)
<i>Pandoravirus celtis</i>	MK174290	2,028,440	93% (1128/1203)
<i>Pandoravirus quercus</i>	NC_037667	2,077,288	93% (1125/1203)
<i>Pandoravirus inopinatum</i>	NC_026440	2,243,109	93% (1133/1203)
<i>Pandoravirus dulcis</i>	NC_021858	1,908,524	92% (1122/1203)
<i>Pandoravirus neocaledonia</i>	NC_037666	2,003,191	86% (1045/1203)
<i>Pandoravirus macleodensis</i>	NC_037665	1,838,258	86% (1039/1203)
<i>Pandoravirus lena</i> (strain DY0)	OQ411594-OQ411599	2,030,260 (6)	93% (1131/1203)
<i>Pandoravirus duvanny</i> (strain DY1)	-	unassembled	92% (1114/1203)
<i>Pandoravirus talik</i> (strain Y4)	OQ413801	1,817,546 (1)	92% (1114/1203)
<i>Pandoravirus mammoth</i> (strain Yana14)	-	not yet sequenced	91% (1104/1203)
<i>Pandoravirus yedoma</i> (strain Y2)	-	not yet sequenced	91% (1095/1203)
<i>Pandoravirus lupus</i> (strain Tums1)	-	not yet sequenced	91% (1092/1203)
<i>Pandoravirus mammoth</i> (strain Mm38)	OQ411600-OQ411601	1,776,082 (2)	86% (1040/1203)

* Computed from the pairwise alignment of various amplicon nucleotide sequences with that of the reference sequence in *P. salinus*. New isolates are indicated in bold.

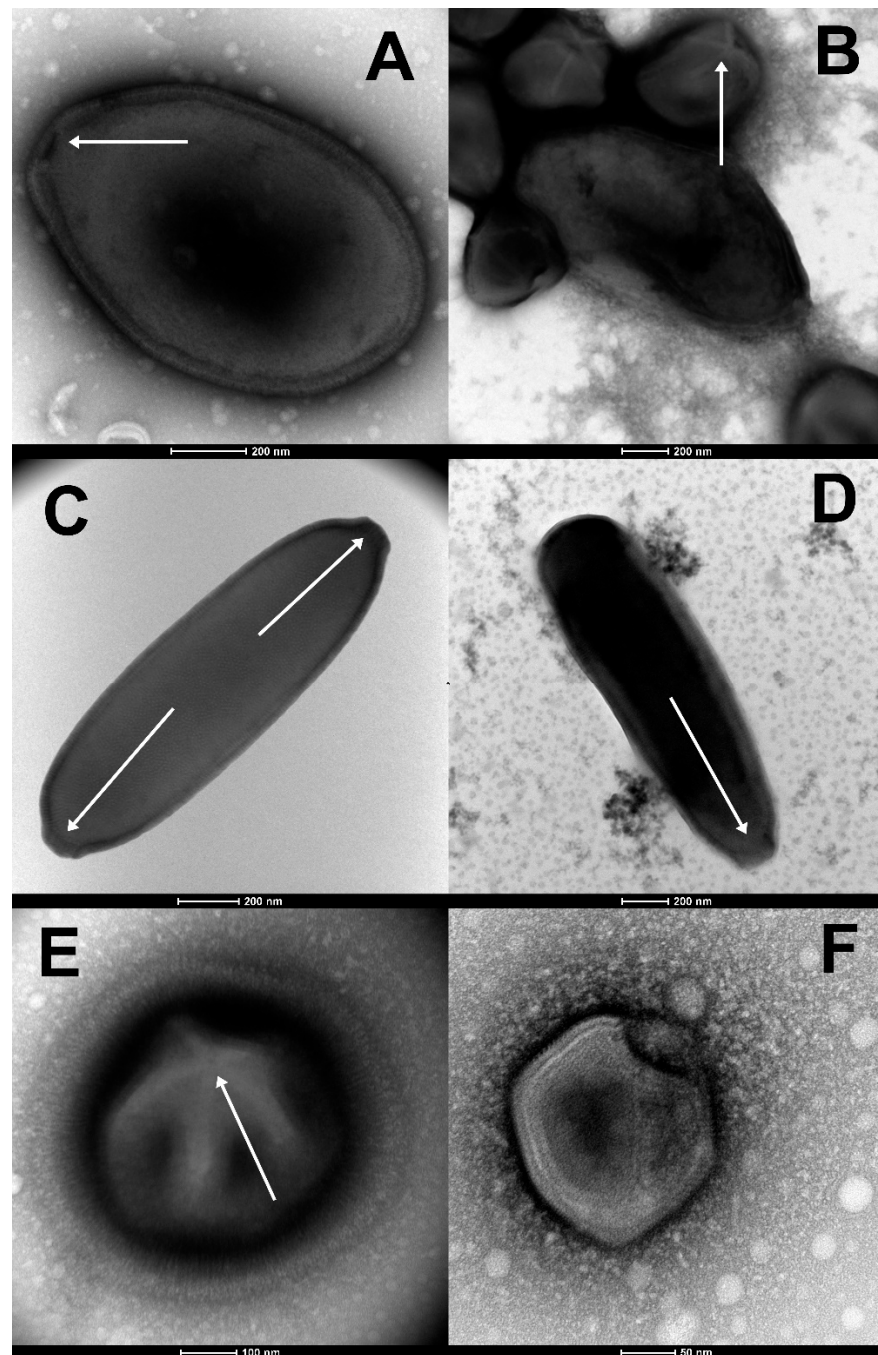


Figure 1. Morphological features guiding the preliminary identification of newly isolated viruses (negative staining, TEM). (A) The large ovoid particle (1000 nm in length) of *Pandoravirus yedoma* (strain Y2) (sample #5 in Table 1) showing the apex ostiole (white arrowhead) and the thick tegument characteristic of the *Pandoraviridae* family. (B) A mixture of *Pandoravirus mammoth* (strain Yana14) oblate particles and of *Megavirus mammoth* (strain Yana14) icosahedral particles exhibiting a “stargate” (white starfish-like structure crowning a vertex, white arrowhead) as seen in sample #7 (Table 1). (C) The elongated particle of *Cedratovirus lena* (strain DY0) (1500 nm in length) exhibits two apex cork-like structures (white arrowheads) (sample #2, Table 1). (D) The elongated particle of *Pithovirus mammoth* (1800 nm in length) (sample #7, Table 1) exhibiting a single apex cork-like structure (white arrowhead). (E) The large (770 nm in diameter) “hairy” icosahedral particle of *Megavirus mammoth* (strain Yana14), showing the “stargate” (white arrowhead) characteristic of the *Megavirinae* subfamily (sample #7, Table 1). (F) The smaller icosahedral particle (200 nm in diameter) of *Pacmanvirus lupus* (strain Tums2) (sample #9, Table 1) typical of asfarviruses/pacmanviruses.

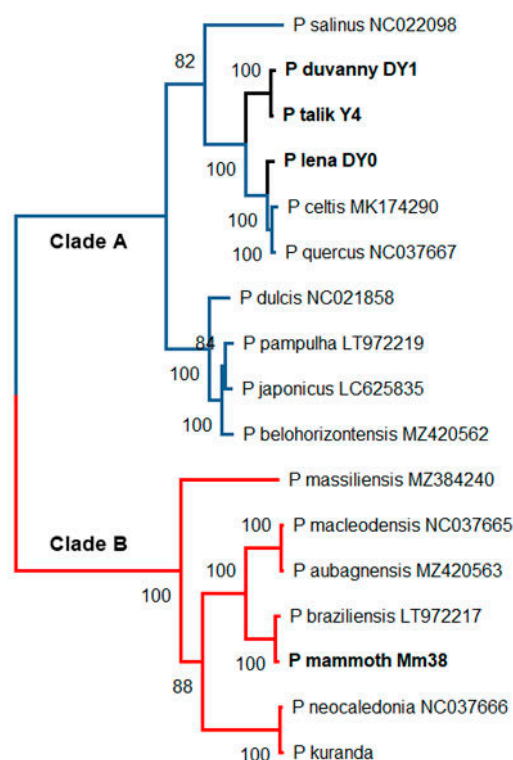


Figure 2. Maximum-likelihood phylogenetic relationships of the available Pandoravirus isolates. The tree (rooted at midpoint) was built using IQ-TREE (version 1.6.2) [54] from 2067 gap-free sites in the multiple alignment of 17 RNA polymerases (RPB1) protein (best fit model: “JTT + F + I + G4”). The permafrost isolates (in bold) are distributed between the two separate *Pandoraviridae* clades previously documented [55]. Accession numbers are indicated following the isolate name when available.

3.2. Cedratvirus and Pithovirus Isolates

Three of the newly isolated viruses belong to the recently proposed “Cedratvirus” clade [56,57] (a new genus or a new subfamily), within the Pithoviridae family [57]. One (Cedratvirus lena (strain DY0)) was cultivated from the same Lena river sample previously cited (sample #2, Table 1), one (Cedratvirus kamchatka (strain P5)) from surface cryosol in Kamchatka collected during the summer (sample #1, Table 1), and one (Cedratvirus duvanny (strain DY1)) from mud flowing into the Kolyma river at Duvanny yar, resulting from the thawing of permafrost layers of mixed ages (sample #4, Table 1). One additional member of the Pithoviridae (*Pithovirus mammoth* (strain Yana14)) was isolated from a 27,000-y old permafrost sample containing a large amount of mammoth wool (sample #7, Table 1). It is worth recalling that the prototype of this family was previously isolated from an ancient permafrost layer of more than 30,000-y BP [41]. Other members of this family are the most abundant in a recent metagenomic study of various Siberian permafrost samples focusing on eukaryotic viruses [58].

We recognized the new Cedratvirus and Pithovirus strains by their large ovoid particles, more elongated (up to 2 μm in length) than those of pandoravirus, with a much thinner wall, and their characteristic terminal cork-like structures (often two on each side for cedraviruses particles) [56,57] (Figure 1C,D). As previously described cedraviruses/pithoviruses, the new isolates enter the *Acanthamoeba* cells by phagocytosis. After ~12 h of infection, mature viral particles were released by cell lysis. As previously noticed [41], the cell nucleus maintained its shape throughout the entire replication cycles.

In complement to these visual clues, PCR tests were performed to confirm the identification of the new isolates using two different clade-specific sets of primers (Table 2) and the amplicons sequenced to evaluate their genetic divergence with known members of the family (Table 4). All new isolates were found to be significantly distinct from each

other and from contemporary strains, but within a range of divergence (94–87%) consistent with that of previously characterized members of these clades (Table 4). In addition, we sequenced the genomes of the three new isolates.

Table 4. PCR identification of previous and newly Cedratvirus and Pithovirus isolates.

Virus	Accession #	Base Pairs	Amplicon Identity *
<i>Cedratvirus A11</i> (prototype)	NC_032108	589,068	100% (1239/1239)
<i>Cedratvirus lausannensis</i>	LT907979	575,161	94% (1176/1239)
<i>Cedratvirus kamchatka</i>	MN873693	466,767	88% (1091/1239)
<i>Cedratvirus lena</i> (strain DY0)	OQ413577-OQ413579, OQ41358	465,544	87% (1090/1239)
<i>Cedratvirus duvanny</i> (strain DY1)	OQ413581	472,117	87% (1087/1239)
<i>Pithovirus sibericum</i> (P1084-T)	NC_023423	610,033	100% (593/593)
<i>Pithovirus mammoth</i> (strain Yana14)	OQ413582	610,309	97% (581/593)

* Computed from the pairwise alignment of various amplicon nucleotide sequences with that of the reference sequence in *Cedratvirus A11*. New isolates are indicated in bold.

3.3. *Megavirus mammoth*

Megavirus mammoth (strain Yana14) is the first Mimiviridae family [59–61] member ever rescued from ancient permafrost. It was isolated from the highly productive sample (dated >27,000-y BP) exhibiting fossil mammoth wool (sample #7, Table 1) together with two other viruses: *Pithovirus mammoth* (Yana14) and *Pandoravirus mammoth* (Yana14).

The particles of *M. mammoth* (strain Yana14) exhibit all the morphological features characteristic of a member of subfamily Megavirinae: a large icosahedral capsid of about 0.5 µm in diameter, surrounded by an external layer of dense fibrils (up to 125 nm thick) (Figure 1E) [59,60]. These features (icosahedral symmetry, large size, fibrils, and stargate) are unique to Mimiviridae members, making their identification straightforward and unambiguous [62].

As previously described members of the Megavirinae subfamily [61], the *M. mammoth* particles enter host cells by phagocytosis. Six to eight hours p.i., infected cells start rounding and losing adherence. New particles are then produced in very large cytoplasmic viral factories, leaving the cell nucleus intact. New virions are then released in large quantities (burst size ≈ 500) through cell lysis.

In complement to the above unambiguous observations, a PCR tests was performed to confirm the identification of the new isolate using a Megavirinae-specific set of primers (Table 2) and the amplicon sequenced to evaluate its genetic divergence with known members of the family. *M. mammoth* was found to be a very close relative of the modern prototype *M. chilensis* (Table 5). Such very low levels of divergence are actually customary within the *Megavirus* genus (also referred to as the C-clade Megavirinae) [63]. A draft sequence of the *M. mammoth* (strain Yana14) genome was determined. A survey of this sequence shows that it encodes all the trademark proteins of the *Megavirus* genus [61]: the MutS-like DNA mismatch repair enzyme (ORF 570, 99% identical residues), the glutamine-dependent asparagine synthetase (ORF 434, 98% identical residues), and the 5 amino-acyl tRNA ligase: Ileu AARS (ORF 383, 99% ID), Asp AARS (ORF 771, 100% ID), Met AARS (ORF 798, 99% ID), Arg AARS (ORF 834, 99% ID), Cys AARS (ORF 837, 98% ID), Trp AARS (ORF 876, 96% ID), and Tyr AARS (ORF 944, 97% ID).

Table 5. PCR identification of Megavirus mammoth (strain Yana14) as a Megavirinae member.

Virus	Accession #	Base Pairs	Amplicon Identity *
<i>Megavirus chilensis</i>	NC_016072	1,259,197	100% (1497/1497)
<i>Megavirus vitis</i>	MG807319	1,242,360	99% (1493/1497)
<i>Megavirus mammoth (strain Yana14)</i>	OQ411602	1,260,651	99% (1493/1497)
<i>Megavirus powai lake</i>	KU877344	1,208,707	93% (1396/1497)
<i>Megavirus baoshan</i>	MH046811	1,224,839	92% (1379/1497)
<i>Moumouvirus</i>	NC_020104	1,021,348	83% (1248/1497)
<i>Moumouvirus australiensis</i>	MG807320	1,098,002	82% (1244/1497)
<i>Mimivirus</i>	NC_014649	1,181,549	77% (1158/1497)

* Computed from the pairwise alignment of various amplicon nucleotide sequences with that of the reference sequence in *Megavirus chilensis*. The new isolate is indicated in bold.

3.4. Pacmanvirus lupus

Pacmanvirus is a clade of recently discovered *Acanthamoeba*-infecting viruses distantly related to the African swine fever virus, until then the only known members of the *Asfarviridae* family that infects pigs [64]. We now report the isolation of a third member of this newly defined group from the frozen intestinal remains of a Siberian wolf (*Canis lupus*) preserved in a permafrost layer dated >27,000-y BP. At variance with the other truly giant viruses (i.e., exhibiting unusually large particles), their icosahedral virions are about 220 nm in diameter (Figure 1F), hence not individually discernable under the light microscope (Nomarski optic). In absence of recognizable specific features, *Pacmanvirus lupus* (strain Tums2) was initially identified by PCR using a specific set of primers (Table 2) and a survey of its draft genomic sequence.

Pacmanvirus lupus genome consists of a double-stranded DNA linear molecule of 407,705 bp, comparable in size to that of the previously studied members of this group (Table 6). However, out of its 506 predicted protein-coding genes, only 241 (47.6%) exhibit homologs in the two previously sequenced *Pacmanvirus* genomes, and 221 (43.7%) are ORFans. Thus, if *Pacmanvirus lupus* appears closer to pacmanviruses than to any other known viruses, its evolutionary distance is larger than usually observed within a subfamily or a genus. This large discrepancy in global gene content is consistent with the low similarity observed between various core genes of *Pacmanvirus lupus* and their homologs in other pacmanviruses and closest relatives (Table 7). The asfarviruses appear even more distant with half the number of genes and half the genome size, perhaps calling for a little more caution before definitely classifying pacmanviruses within the *Asfarviridae* (Table 7) [64]. Based on a comparison of RPB1 orthologs, *P. lupus* appears unambiguously clustered with other known members of genus *Pacmanvirus* (hence justifying its name) (Figure 3).

Table 6. PCR Identification of *Pacmanvirus lupus* (strain Tums2) as a new member of genus *Pacmanvirus*.

Virus	Accession #	Base Pairs	Amplicon Identity *
<i>Pacmanvirus A23</i>	NC_034383	395,405	100% (470/470)
<i>Pacmanvirus S19</i>	MZ440852	418,588	93% (439/470)
<i>Pacmanvirus lupus (strain Tums2)</i>	OQ411603	407,705	<85% (399/468) + two large insertions

* Computed from the pairwise alignment of various amplicon nucleotide sequences with that of the reference sequence in *Pacmanvirus A23*. The new isolate is indicated in bold.

Table 7. Closest virus relatives of *Pacmanvirus lupus*.

<i>Pacmanvirus lupus</i> Predicted Protein	<i>Pacmanvirus A23</i> NC_034383 %ID (aa)	<i>Pacmanvirus S19</i> MZ440852 %ID (aa)	<i>Faustovirus</i> KJ614390 %ID (aa)	<i>Kaumobavirus</i> NC_034249 %ID (aa)	<i>Asfarviruses</i> NC_044958 %ID (aa)
RNA polymerase (RPB1) ORF 302	79% (1124/1415)	80% (1130/1415)	49% (707/1434)	42% (598/1429)	41% (596/1457)
RNA polymerase (RPB2) ORF 33	85% (1093/1289)	85% (1104/1301)	55% (681/1241)	44% (528/1211)	43% (526/1228)
DNA polymerase (PolB) ORF 265	65% (1036/1591)	65% (1032/1591)	37% (513/1385)	27.5% (344/1250)	33% (382/1163)
Genome size					
407,705 bp	395,405 bp	418,588 bp	457–491 kb	351–363 kb	172–191 kb

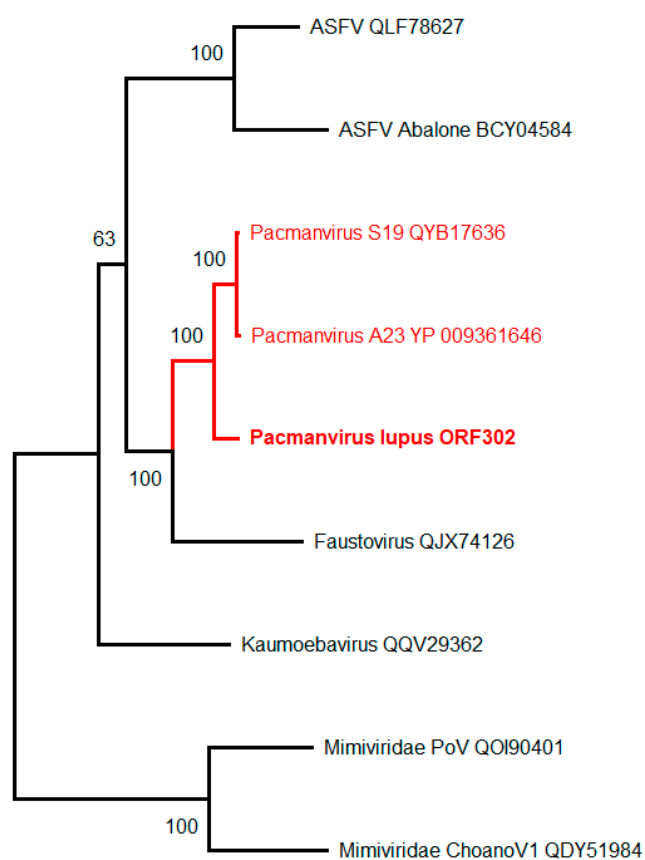


Figure 3. Maximum-likelihood phylogenetic relationships of the closest *Pacmanvirus lupus* relatives (using RPB1 homologs, Table 7). The tree (rooted at midpoint) was built using IQ-TREE (version 1.6.2) [54] (best fit model: “LG + F + I + G4”). The two closest *Mimiviridae* RPB1 sequences are used as an outgroup. The tree was built from 1314 gap-free sites in the multiple alignment of 9 RNA polymerases (RPB1) protein sequences. Although *Pacmanvirus lupus* is well clustered with other pacmanviruses, this clade (together with faustovirus) appears more as a sister group rather than *bona fide* members within the *Asfarviridae* (ASFV) family. Accession numbers are indicated following the isolate name when available.

4. Discussion

Following initial reports published more than five years ago [41,42], this study confirms the capacity of large DNA viruses infecting *Acanthamoeba* to remain infectious after more than 48,500 years spent in deep permafrost. Moreover, our results extend our previous findings to three additional virus families or groups: four new members of the

Pandoraviridae, one member of the *Mimiviridae*, and one pacmanvirus (Table 1). One additional pithovirus was also revived from a particularly productive sample dated 27,000-y BP (sample#7, Table 1) exhibiting mammoth wool. Given these viruses' diversity both in their particle structure and replication mode, one can reasonably infer that many other eukaryotic viruses infecting a variety of hosts much beyond *Acanthamoeba* spp. may also remain infectious in similar conditions. Genomic traces of such viruses were detected in a recent large-scale metagenomic study of ancient permafrost [58] as well as in Arctic lake sediments [65]. They include well-documented human and vertebrate pathogens such as poxviruses, herpesviruses, and asfarviruses, although in lower proportions than protozoan infecting viruses.

In our recent metagenomic study [58], pandoraviruses are notably absent while they constitute the large majority of the viruses revived from permafrost and cryosols. Such a discrepancy might originate from the fact that the extraction of genomic DNA from their sturdy particles requires a much harsher treatment than for most other viruses. Their abundance in environmental viromes might thus be much larger than the small fraction they contribute to the DNA pool. Such DNA extraction bias may apply to many other microbes, and is a serious limitation to the validity of metagenomic approaches for quantitative population studies.

The types of viruses revived in our study are indeed the results of even stronger biases. First, the only viruses we can expect to detect are those infecting species of *Acanthamoeba*. Second, because we rely on "sick" amoeba to point out potentially virus-replicating cultures, we strongly limit ourselves to the detection of lytic viruses. Third, we favor the identification of "giant" viruses, given the important role given to light microscopy in the early detection of positive viral cultures. It is thus likely that many small, non-lytic viruses do escape our scrutiny, as well as those infecting many other protozoa that can survive in ancient permafrost [10].

However, we believe that the use of *Acanthamoeba* cells as a virus bait is nevertheless a good choice for several reasons. First, *Acanthamoeba* spp. are free-living amoebae that are ubiquitous in natural environments, such as soils and fresh, brackish, and marine waters, but are also in dust particles, pools, water taps, sink drains, flowerpots, aquariums, sewage, as well as in medical settings (hydrotherapy baths, dental irrigation equipment, humidifiers, cooling systems, ventilators, and intensive care units) [66]. The detection of their viruses may thus provide a useful test for the presence of any other live viruses in a given setting. Second, if many *Acanthamoeba* species can be conveniently propagated in axenic culture conditions, they remain "self-cleaning" thanks to phagocytosis, and are capable of tolerating heavy contamination by bacteria (that they eat) as well as high doses of antibiotics and antifungals. The third, but not the smallest, advantage is that of biological security. When we use *Acanthamoeba* spp. cultures to investigate the presence of infectious unknown viruses in prehistorical permafrost (in particular from paleontological sites, such as RHS [46,47]), we are using its billion years of evolutionary distance with human and other mammals as the best possible protection against an accidental infection of laboratory workers or the spread of a dreadful virus once infecting Pleistocene mammals to their contemporary relatives. The biohazard associated with reviving prehistorical amoeba-infecting viruses is thus totally negligible compared to the search for "paleoviruses" directly from permafrost-preserved remains of mammoths, woolly rhinoceros, or prehistoric horses, as it is now pursued in the Vector laboratory (Novosibirsk, Russia) [67], fortunately a BSL4 facility. Without the need to embark on such a risky project, we believe our results with *Acanthamoeba*-infecting viruses can be extrapolated to many other DNA viruses capable of infecting humans or animals. It is thus likely that ancient permafrost (eventually much older than 50,000 years, our limit solely dictated by the validity range of radiocarbon dating) will release these unknown viruses upon thawing. How long these viruses could remain infectious once exposed to outdoor conditions (UV light, oxygen, heat), and how likely they will be to encounter and infect a suitable host in the interval, is yet impossible to estimate, but the risk is bound to increase in the context of global warming, in which

permafrost thawing will keep accelerating, and more people will populate the Arctic in the wake of industrial ventures.

Author Contributions: Conceptualization and funding, C.A. and J.-M.C.; resources (samples), A.E.G., G.G., J.S., A.N.F. and A.N.T.; virus isolation and characterization: J.-M.A. and A.L.; bioinformatic analysis, O.P., M.L., S.S. and J.-M.C.; writing, J.-M.C.; All authors have read and agreed to the published version of the manuscript.

Funding: This work was supported by the Agence Nationale de la Recherche grant (ANR-10-INBS-09-08) to J-MC, the CNRS Projet de Recherche Conjoint (PRC) grant (PRC1484-2018) to CA, the European Research Council (ERC) under the European Union's Horizon 2020 research and innovation program (grant agreement No 832601) to C.A., and the recurrent CNRS funding to the IGS laboratory. GG and JS were funded by a European Research Council starting grant (PETA-CARB, #338335) and the Helmholtz Association of German Research Centres (HGF) Impulse and Networking Fund (ERC-0013).

Institutional Review Board Statement: Not Applicable.

Informed Consent Statement: Not Applicable.

Data Availability Statement: The newly isolated viruses described here are available for collaborative studies upon formal request through a material transfer agreement.

Acknowledgments: We thank Maksim Cheprasov (NEFU, Yakutsk, Russia) and Vladimir Pitulko (RAS, St Petersburg, Russia) for their generous gift of ancient permafrost samples. We also thank our volunteer collaborator, Alexander Morawitz, for collecting the Kamchatka soil samples and Lyubov Shmakova (Soil Cryology Lab, Pushchino, Russia) for providing samples from which, unfortunately, no viruses were rescued in the present study. We thank Sofia Rigou for assembling the C. lena and C. duvanny genomes and we acknowledge the computing support of the PACA BioInfo platform. We thank M. Ulrich (DFG project #UL426/1-1) and P. Konstantinov for helping with fieldwork at the Yukechi site, as well as the Alfred Wegener Institute and Melnikov Permafrost Institute logistics for field support and sample acquisition.

Conflicts of Interest: The authors declare no conflict of interest.

References

1. IPCC. 2022: *Climate Change 2022: Impacts, Adaptation and Vulnerability. Contribution of Working Group II to the Sixth Assessment Report of the Intergovernmental Panel on Climate Change*; Pörtner, H.-O., Roberts, D.C., Tignor, M., Poloczanska, E.S., Mintenbeck, K., Alegría, A., Craig, M., Langsdorf, S., Lösschke, S., Möller, V., Okem, A., Rama, B., Eds.; Cambridge University Press: Cambridge, UK; New York, NY, USA, 2022; 3056p. [[CrossRef](#)]
2. Palmer, T.; Stevens, B. The scientific challenge of understanding and estimating climate change. *Proc. Natl. Acad. Sci. USA* **2019**, *116*, 24390–24395. [[CrossRef](#)]
3. Rantanen, M.; Karpechko, A.Y.; Lipponen, A.; Nordling, K.; Hyvärinen, O.; Ruosteenoja, K.; Vihma, T.; Laaksonen, A. The Arctic has warmed nearly four times faster than the globe since 1979. *Commun. Earth Environ.* **2022**, *3*, 168. [[CrossRef](#)]
4. Biskaborn, B.K.; Smith, S.L.; Noetzi, J.; Matthes, H.; Vieira, G.; Streletskiy, D.A.; Schoeneich, P.; Romanovsky, V.E.; Lewkowicz, A.G.; Abramov, A.; et al. Permafrost is warming at a global scale. *Nat. Commun.* **2019**, *10*, 264. [[CrossRef](#)]
5. Turetsky, M.R.; Abbott, B.W.; Jones, M.C.; Walter Anthony, K.; Olefeldt, D.; Schuur, E.A.; Koven, C.; McGuire, A.D.; Grosse, G.; Kuhry, P.; et al. Permafrost collapse is accelerating carbon release. *Nature* **2019**, *569*, 32–44. [[CrossRef](#)]
6. Fuchs, M.; Nitze, I.; Strauss, J.; Günther, F.; Wetterich, S.; Kizyakov, A.; Fritz, M.; Opel, T.; Grigoriev, M.N.; Maksimov, G.T.; et al. Rapid fluvio-thermal erosion of a yedoma permafrost cliff in the Lena River Delta. *Front. Earth Sci.* **2020**, *8*, 336. [[CrossRef](#)]
7. Günther, F.; Overduin, P.P.; Sandakov, A.V.; Grosse, G.; Grigoriev, M.N. Short- and long-term thermo-erosion of ice-rich permafrost coasts in the Laptev Sea region. *Biogeosciences* **2013**, *10*, 4297–4318. [[CrossRef](#)]
8. Murton, J.B.; Opel, T.; Toms, P.; Blinov, A.; Fuchs, M.; Wood, J.; Gartner, A.; Merchel, S.; Rugel, G.; Savvinov, G.; et al. A multimethod dating study of ancient permafrost, Batagay megaslump, East Siberia. *Quat. Res.* **2022**, *105*, 1–22. [[CrossRef](#)]
9. Kizyakov, A.I.; Wetterich, S.; Günther, F.; Opel, T.; Jongejans, L.L.; Courtin, J.; Meyer, H.; Shepelev, A.G.; Syromyatnikov, I.I.; Fedorov, A.N.; et al. Landforms and Degradation Pattern of the Batagay Thaw Slump, Northeastern Siberia. *Geomorphology* **2023**, *420*, 108501. [[CrossRef](#)]
10. Gilichinsky, D.; Wagener, S. Microbial life in permafrost: A historical review. *Permafrost Periglacial Process.* **1995**, *6*, 243–250. [[CrossRef](#)]
11. Burkert, A.; Douglas, T.A.; Waldrop, M.P.; Mackelprang, R. Changes in the Active, Dead, and Dormant Microbial Community Structure across a Pleistocene Permafrost Chronosequence. *Appl. Environ. Microbiol.* **2019**, *85*, e02646-18. [[CrossRef](#)]

12. Hultman, J.; Waldrop, M.; Mackelprang, R.; David, M.M.; McFarland, J.; Blazewicz, S.J.; Harden, J.; Turetsky, M.R.; McGuire, A.D.; Shah, M.B.; et al. Multi-omics of permafrost, active layer and thermokarst bog soil microbiomes. *Nature* **2015**, *521*, 208–212. [[CrossRef](#)]
13. Malavin, S.; Shmakova, L.; Claverie, J.-M.; Rivkina, E. Frozen Zoo: A collection of permafrost samples containing viable protists and their viruses. *Biodivers. Data J.* **2020**, *8*, e51586. [[CrossRef](#)]
14. Lydolph, M.C.; Jacobsen, J.; Arctander, P.; Gilbert, M.T.; Gilichinsky, D.A.; Hansen, A.J.; Willerslev, E.; Lange, L. Beringian paleoecology inferred from permafrost-preserved fungal DNA. *Appl. Environ. Microbiol.* **2005**, *71*, 1012–1017. [[CrossRef](#)]
15. Mishra, U.; Hugelius, G.; Shelef, E.; Yang, Y.; Strauss, J.; Lupachev, A.; Harden, J.W.; Jastrow, J.D.; Ping, C.L.; Riley, W.J.; et al. Spatial heterogeneity and environmental predictors of permafrost region soil organic carbon stocks. *Sci. Adv.* **2021**, *7*, eaaz5236. [[CrossRef](#)]
16. Walter, K.M.; Zimov, S.A.; Chanton, J.P.; Verbyla, D.; Chapin, F.S., 3rd. Methane bubbling from Siberian thaw lakes as a positive feedback to climate warming. *Nature* **2006**, *443*, 71–75. [[CrossRef](#)]
17. Vishnivetskaya, T.A.; Petrova, M.A.; Urbance, J.; Ponder, M.; Moyer, C.L.; Gilichinsky, D.A.; Tiedje, J.M. Bacterial community in ancient Siberian permafrost as characterized by culture and culture-independent methods. *Astrobiology* **2006**, *6*, 400–414. [[CrossRef](#)]
18. Johnson, S.S.; Hebsgaard, M.B.; Christensen, T.R.; Mastepanov, M.; Nielsen, R.; Munch, K.; Brand, T.; Gilbert, M.T.; Zuber, M.T.; Bunce, M.; et al. Ancient bacteria show evidence of DNA repair. *Proc. Natl. Acad. Sci. USA* **2007**, *104*, 14401–14405. [[CrossRef](#)]
19. Revich, B.A.; Podolnaya, M.A. Thawing of permafrost may disturb historic cattle burial grounds in East Siberia. *Glob. Health Action* **2011**, *4*, 8482. [[CrossRef](#)]
20. Hueffer, K.; Drown, D.; Romanovsky, V.; Hennessy, T. Factors contributing to anthrax outbreaks in the circumpolar north. *Ecohealth* **2020**, *17*, 174–180. [[CrossRef](#)]
21. Timofeev, V.; Bahtejeva, I.; Mironova, R.; Titareva, G.; Lev, I.; Christiany, D.; Borzilov, A.; Bogun, A.; Vergnaud, G. Insights from *Bacillus anthracis* strains isolated from permafrost in the tundra zone of Russia. *PLoS ONE* **2019**, *14*, e0209140. [[CrossRef](#)]
22. Legostaeva, Y.; Gololobova, A.; Popov, V. Geochemical Risks of Diamond Mining in Siberia. *Environ. Sci. Proc.* **2021**, *5*, 4. [[CrossRef](#)]
23. Murton, J.B.; Goslar, T.; Edwards, M.E.; Bateman, M.D.; Danilov, P.P.; Savvinov, G.N.; Gubin, S.V.; Ghaleb, B.; Haile, J.; Kanevskiy, M.; et al. Palaeoenvironmental Interpretation of Yedoma Silt (Ice Complex) Deposition as Cold-Climate Loess, Duvanny Yar, Northeast Siberia. *Permafrost Periglacial Process.* **2015**, *26*, 208–288. [[CrossRef](#)]
24. Mackelprang, R.; Waldrop, M.P.; DeAngelis, K.M.; David, M.M.; Chavarría, K.L.; Blazewicz, S.J.; Rubin, E.M.; Jansson, J.K. Metagenomic analysis of a permafrost microbial community reveals a rapid response to thaw. *Nature* **2011**, *480*, 368–371. [[CrossRef](#)]
25. Krivushin, K.; Kondrashov, F.; Shmakova, L.; Tutukina, M.; Petrovskaya, L.; Rivkina, E. Two metagenomes from late pleistocene northeast siberian permafrost. *Genome Announc.* **2015**, *3*, e01380-14. [[CrossRef](#)]
26. Perron, G.G.; Whyte, L.; Turnbaugh, P.J.; Goordial, J.; Hanage, W.P.; Dantas, G.; Desai, M.M. Functional characterization of bacteria isolated from ancient arctic soil exposes diverse resistance mechanisms to modern antibiotics. *PLoS ONE* **2015**, *10*, e0069533. [[CrossRef](#)]
27. Mackelprang, R.; Burkert, A.; Haw, M.; Mahendrarajah, T.; Conaway, C.H.; Douglas, T.A.; Waldrop, M.P. Microbial survival strategies in ancient permafrost: Insights from metagenomics. *ISME J.* **2017**, *11*, 2305–2318. [[CrossRef](#)]
28. Taş, N.; Prestat, E.; Wang, S.; Wu, Y.; Ulrich, C.; Kneafsey, T.; Tringe, S.G.; Torn, M.S.; Hubbard, S.S.; Jansson, J.K. Landscape topography structures the soil microbiome in arctic polygonal tundra. *Nat. Commun.* **2018**, *9*, 777. [[CrossRef](#)]
29. Liang, R.; Lau, M.; Vishnivetskaya, T.; Lloyd, K.G.; Wang, W.; Wiggins, J.; Miller, J.; Pfiffner, S.; Rivkina, E.M.; Onstott, T.C. Predominance of Anaerobic, Spore-Forming Bacteria in Metabolically Active Microbial Communities from Ancient Siberian Permafrost. *Appl. Environ. Microbiol.* **2019**, *85*, e00560-19. [[CrossRef](#)]
30. Abramov, A.; Vishnivetskaya, T.; Rivkina, E. Are permafrost microorganisms as old as permafrost? *FEMS Microbiol. Ecol.* **2021**, *97*, fiae260. [[CrossRef](#)]
31. Rigou, S.; Christo-Foroux, E.; Santini, S.; Goncharov, A.; Strauss, J.; Grosse, G.; Fedorov, A.N.; Labadie, K.; Abergel, C.; Claverie, J.M. Metagenomic survey of the microbiome of ancient Siberian permafrost and modern Kamchatkan cryosols. *microLife* **2022**, *3*, uqac003. [[CrossRef](#)]
32. Walsh, C.; Wenciewicz, T. *Antibiotics: Challenges, Mechanisms, Opportunities*, 2nd ed.; John Wiley & Sons: Hoboken, NJ, USA, 2020.
33. Haan, T.J.; Drown, D.M. Unearthing antibiotic resistance associated with disturbance-induced permafrost thaw in interior Alaska. *Microorganisms* **2021**, *9*, 116. [[CrossRef](#)]
34. De Cock, K.M.; Jaffe, H.W.; Curran, J.W. Reflections on 40 Years of AIDS. *Emerg. Infect. Dis.* **2021**, *27*, 1553–1560. [[CrossRef](#)]
35. Miranda, M.N.S.; Pingarilho, M.; Pimentel, V.; Torneri, A.; Seabra, S.G.; Libin, P.J.K.; Abecasis, A.B. A Tale of Three Recent Pandemics: Influenza, HIV and SARS-CoV-2. *Front. Microbiol.* **2022**, *13*, 889643. [[CrossRef](#)]
36. Nasir, A.; Romero-Severson, E.; Claverie, J.-M. Investigating the Concept and Origin of Viruses. *Trends Microbiol.* **2020**, *28*, 959–967. [[CrossRef](#)]
37. Claverie, J.-M. Fundamental Difficulties Prevent the Reconstruction of the Deep Phylogeny of Viruses. *Viruses* **2020**, *12*, 1130. [[CrossRef](#)]

38. Emerson, J.B.; Roux, S.; Brum, J.R.; Bolduc, B.; Woodcroft, B.J.; Jang, H.B.; Singleton, C.M.; Solden, L.M.; Naas, A.E.; Boyd, J.A.; et al. Host-linked soil viral ecology along a permafrost thaw gradient. *Nat. Microbiol.* **2018**, *3*, 870–880. [[CrossRef](#)]
39. Reid, A.H.; Fanning, T.G.; Hultin, J.V.; Taubenberger, J.K. Origin and evolution of the 1918 "Spanish" influenza virus hemagglutinin gene. *Proc. Natl. Acad. Sci. USA* **1999**, *96*, 1651–1656. [[CrossRef](#)]
40. Biagini, P.; Thèves, C.; Balaesque, P.; Géraud, A.; Cannet, C.; Keyser, C.; Nikolaeva, D.; Gérard, P.; Duchesne, S.; Orlando, L.; et al. Variola virus in a 300-year-old Siberian mummy. *N. Engl. J. Med.* **2012**, *367*, 2056–2058. [[CrossRef](#)]
41. Legendre, M.; Bartoli, J.; Shmakova, L.; Jeudy, S.; Labadie, K.; Adrait, A.; Lescot, M.; Poirot, O.; Bertaux, L.; Bruley, C.; et al. Thirty-thousand-year-old distant relative of giant icosahedral DNA viruses with a Pandoravirus morphology. *Proc. Natl. Acad. Sci. USA* **2014**, *111*, 4274–4279. [[CrossRef](#)]
42. Legendre, M.; Lartigue, A.; Bertaux, L.; Jeudy, S.; Bartoli, J.; Lescot, M.; Alempic, J.-M.; Ramus, C.; Bruley, C.; Labadie, K.; et al. In-depth study of Mollivirus sibericum, a new 30,000-y-old giant virus infecting Acanthamoeba. *Proc. Natl. Acad. Sci. USA* **2015**, *112*, E5327–E5335. [[CrossRef](#)]
43. Jongejans, L.L.; Grosse, G.; Ulrich, M.; Fedorov, A.N.; Konstantinov, P.; Strauss, J. Radiocarbon ages of talik sediments of an alask lake and a yedoma lake in the Yukechi Alas, Siberia. *PANGAEA* **2019**. [[CrossRef](#)]
44. Shmelev, D.; Cherbunina, M.; Rogov, V.; Opfergelt, S.; Monhonval, A.; Strauss, J. Reconstructing Permafrost Sedimentological Characteristics and Post-depositional Processes of the Yedoma Stratotype Duvanny Yar, Siberia. *Front. Earth Sci.* **2021**, *9*, 727315. [[CrossRef](#)]
45. Grigoriev, S.E.; Fisher, D.C.; Obadã, T.; Shirley, E.A.; Rountrey, A.N.; Savvinov, G.N.; Darima, K.; Garmaeva, D.K.; Novgorodov, G.P.; Cheprasov, M.Y.; et al. A woolly mammoth (*Mammuthus primigenius*) carcass from maly Lyakhovsky island (new siberian islands, Russian Federation). *Quat. Int.* **2017**, *445*, 89–103. [[CrossRef](#)]
46. Pitulko, V.V.; Nikolsky, P.A.; Girya, E.Y.; Basilyan, A.E.; Tumskey, V.E.; Koulakov, S.A.; Astakhov, S.N.; Pavlova, E.Y.; Anisimov, M.A. The Yana RHS site: Humans in the Arctic before the last glacial maximum. *Science* **2004**, *303*, 52–56. [[CrossRef](#)]
47. Basilyan, A.E.; Anisimov, M.A.; Nikolskiy, P.A.; Pitulko, V.V. Woolly mammoth mass accumulation next to the Paleolithic Yana RHS site, Arctic Siberia: Its geology, age, and relation to past human activity. *J. Archaeol. Sci.* **2011**, *38*, 2461–2474. [[CrossRef](#)]
48. Guglielmini, J.; Woo, A.C.; Krupovic, M.; Forterre, P.; Gaia, M. Diversification of giant and large eukaryotic dsDNA viruses predated the origin of modern eukaryotes. *Proc. Natl. Acad. Sci. USA* **2019**, *116*, 19585–19592. [[CrossRef](#)]
49. Christo-Foroux, E.; Alempic, J.-M.; Lartigue, A.; Santini, S.; Labadie, K.; Legendre, M.; Abergel, C.; Claverie, J.-M. Characterization of Mollivirus kamchatka, the First Modern Representative of the Proposed Molliviridae Family of Giant Viruses. *J. Virol.* **2020**, *94*, e01997-19. [[CrossRef](#)]
50. Emms, D.M.; Kelly, S. OrthoFinder: Phylogenetic orthology inference for comparative genomics. *Genome Biol.* **2019**, *20*, 238. [[CrossRef](#)]
51. Suyama, M.; Torrents, D.; Bork, P. PAL2NAL: Robust conversion of protein sequence alignments into the corresponding codon alignments. *Nucleic Acids Res.* **2006**, *34*, W609–W612. [[CrossRef](#)]
52. Eddy, S. show statistics for a multiple alignment file. Available online: <http://pwet.fr/man/linux/commandes/alistat/> (accessed on 30 September 2020).
53. Philippe, N.; Legendre, M.; Doutre, G.; Couté, Y.; Poirot, O.; Lescot, M.; Arslan, D.; Seltzer, V.; Bertaux, L.; Bruley, C.; et al. Pandoraviruses: Amoeba viruses with genomes up to 2.5 Mb reaching that of parasitic eukaryotes. *Science* **2013**, *341*, 281–286. [[CrossRef](#)]
54. Nguyen, L.T.; Schmidt, H.A.; von Haeseler, A.; Minh, B.Q. IQ-TREE: A fast and effective stochastic algorithm for estimating maximum-likelihood phylogenies. *Mol. Biol. Evol.* **2015**, *32*, 268–274. [[CrossRef](#)]
55. Legendre, M.; Alempic, J.M.; Philippe, N.; Lartigue, A.; Jeudy, S.; Poirot, O.; Ta, N.T.; Nin, S.; Couté, Y.; Abergel, C.; et al. Pandoravirus Celtis Illustrates the Microevolution Processes at Work in the Giant Pandoraviridae Genomes. *Front. Microbiol.* **2019**, *10*, 430. [[CrossRef](#)]
56. Andreani, J.; Aherfi, S.; Bou Khalil, J.Y.; Di Pinto, F.; Bitam, I.; Raoult, D.; Colson, P.; La Scola, B. Cedratvirus, a Double-Cork Structured Giant Virus, is a Distant Relative of Pithoviruses. *Viruses* **2016**, *8*, 300. [[CrossRef](#)]
57. Bertelli, C.; Mueller, L.; Thomas, V.; Pilonel, T.; Jacquier, N.; Greub, G. Cedratvirus lausannensis - digging into Pithoviridae diversity. *Environ. Microbiol.* **2017**, *19*, 4022–4034. [[CrossRef](#)]
58. Rigou, S.; Santini, S.; Abergel, C.; Claverie, J.-M.; Legendre, M. Past and present giant viruses diversity explored through permafrost metagenomics. *Nat. Commun.* **2022**, *13*, 5853. [[CrossRef](#)]
59. Raoult, D.; Audic, S.; Robert, C.; Abergel, C.; Renesto, P.; Ogata, H.; La Scola, B.; Suzan, M.; Claverie, J.-M. The 1.2-megabase genome sequence of Mimivirus. *Science* **2004**, *306*, 1344–1350. [[CrossRef](#)]
60. Arslan, D.; Legendre, M.; Seltzer, V.; Abergel, C.; Claverie, J.-M. Distant Mimivirus relative with a larger genome highlights the fundamental features of Megaviridae. *Proc. Natl. Acad. Sci. USA* **2011**, *108*, 17486–17491. [[CrossRef](#)]
61. Claverie, J.-M.; Abergel, C. Mimiviridae: An Expanding Family of Highly Diverse Large dsDNA Viruses Infecting a Wide Phylogenetic Range of Aquatic Eukaryotes. *Viruses* **2018**, *10*, 506. [[CrossRef](#)]
62. Xiao, C.; Kuznetsov, Y.G.; Sun, S.; Hafenstein, S.L.; Kostyuchenko, V.A.; Chipman, P.R.; Suzan-Monti, M.; Raoult, D.; McPherson, A.; Rossmann, M.G. Structural studies of the giant mimivirus. *PLoS Biol.* **2009**, *7*, e92. [[CrossRef](#)]

63. Notaro, A.; Poirot, O.; Garcin, E.D.; Nin, S.; Molinaro, A.; Tonetti, M.; De Castro, C.; Abergel, C. Giant viruses of the Megavirinae subfamily possess biosynthetic pathways to produce rare bacterial-like sugars in a clade-specific manner. *microLife* **2022**, *3*, uqac002. [[CrossRef](#)]
64. Andreani, J.; Khalil, J.Y.B.; Sevvana, M.; Benamar, S.; Di Pinto, F.; Bitam, I.; Colson, P.; Klose, T.; Rossmann, M.G.; Raoult, D.; et al. Pacmanvirus, a New Giant Icosahedral Virus at the Crossroads between Asfarviridae and Faustoviruses. *J. Virol.* **2017**, *91*, e00212-17. [[CrossRef](#)]
65. Lemieux, A.; Colby, G.A.; Poulain, A.J.; Aris-Brosou, S. Viral spillover risk increases with climate change in High Arctic lake sediments. *Proc. Biol. Sci.* **2022**, *289*, 20221073. [[CrossRef](#)]
66. Qvarnstrom, Y.; Nerad, T.A.; Visvesvara, G.S. Characterization of a new pathogenic Acanthamoeba Species, *A. byersi* n. sp., isolated from a human with fatal amoebic encephalitis. *J. Eukaryot. Microbiol.* **2013**, *60*, 626–633. [[CrossRef](#)]
67. Nature World News. Available online: <https://www.natureworldnews.com/articles/45267/20210222/prehistoric-animal-viruses-permafrost-caught-interest-russian-scientists.htm> (accessed on 22 February 2021).

Disclaimer/Publisher’s Note: The statements, opinions and data contained in all publications are solely those of the individual author(s) and contributor(s) and not of MDPI and/or the editor(s). MDPI and/or the editor(s) disclaim responsibility for any injury to people or property resulting from any ideas, methods, instructions or products referred to in the content.